

Numerical Simulation to Get Flow Pattern in Modified Carotid Artery Bifurcation Model Using PIV

Hong Biao¹, Wang Wei¹, Wang Xixu¹, Wang Jue¹, Ye Meng²

¹ Department of Vascular Surgery, Shanghai Tongren Hospital, Shanghai 200050, China

² Department of Vascular Surgery of Renji Hospital, Shanghai Jiaotong University School of Medicine, Shanghai 200127, China
phdman@163.com

Abstract: The aim of this paper was to describe the local flow pattern of carotid bifurcation model using instantaneous velocity fields acquired by particle image velocimetry (PIV) and numerical simulation. Solid modified tuning-fork averaged human carotid bifurcation (TF-AHCB) carotid bifurcation glass model was attached to a circuit driven by different static pressure gradient which produced different velocity. The working fluid consisted of glycerin and water mixture with a viscosity of 3.75mPa. s. Hollow glass spheres with a mean size of 10 μ m were used as tracer particles. Instantaneous velocity fields were obtained by means of PIV and shear stresses were calculated according to the velocity parameters. The same parameters were used for numerical simulation to get the velocity fields and wall shear stress distribution. The results showed that both by PIV and numerical simulation, a large flow separation with an anticlockwise rotating vortex formed at the outside wall of internal carotid artery (ICA) inside the model. The location and scope of the vortex changed with the velocity. The higher the velocity was, the smaller the vortex scope was, and the further the location to the bifurcation was. The flow pattern inside the model consists of large flow separation and anticlockwise vortex zones, the center of which locates near the sinus of ICA and are thought to be associated with the genesis of atherosclerosis.

[Hong B, Wang W, Wang X, Wang J, Ye M. **Numerical Simulation to Get Flow Pattern in Modified Carotid Artery Bifurcation Model Using PIV.** *Life Sci J* 2012;9(3):1296-1301] (ISSN:1097-8135).
<http://www.lifesciencesite.com>.185

Keywords: Numerical simulation; particle image velocimetry (PIV); carotid bifurcation; atherosclerosis

1. Introduction

Nowadays, within the in vitro model study, the carotid artery bifurcation model was one of the most generally used in researching atherosclerosis. The Y shaped averaged human carotid bifurcation had been usually used (Ku et al., 1985; Lee and Chiu, 1995; Rindt and Steenhoven, 1996). Later, Ding et al (2001; 2002) proposed a tuning-fork averaged human carotid bifurcation (TF-AHCB) model. Their study confirmed the stronger correlation between the OSI and intimal thickness in the tuning-fork geometry of human carotid bifurcation. On the basis of TF-AHCB model, Yu et al (2007) modified the parameters to make it more similar to the real geometry.

The PIV technique was a new flow measuring technique which could record all of the relevant information in the whole working section. And it was suitable for the study of complicated flow such as vortex flow and turbulent flow. In this research the time-saving technique-PIV was used to measure the flow fields inside the model. At the same time we use the CAD technique to research the flow fields within the model by numerical simulation as the supplement of PIV research.

2. Material and Methods

The diameter and geometry carotid bifurcation model were listed in Figure1. Its geometry has such requests: The ICA, ECA and CCA are in the same section; The internal carotid artery is straight at least with double lengths of the sinus; All of the cross-sections including the sinus were round; The ICA curves from the end of the sinus, and paralleled with ECA; The bifurcation angle was 45°.

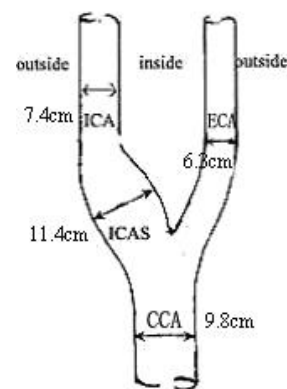


Figure 1. The geometry of the modified TF-AHCB model

The instrument of the circulating was shown in Figure2. The flow velocity was controlled by regulating the water level of the upstream reservoir. The mixture in the downstream reservoir returned into the upstream reservoir with the help of a centrifugal pump. The flow rate was measured by means of an ultrasound flow meter (T206, Transonic Systems, Ithaca, USA).

A solution containing about 35% glycerine (Sigma, USA) and 65% water was used to provide a fluid with a viscosity comparable to blood. The resulting viscosity was measured by means of a capillary viscosimeter (Cavis, Raczek, Wedemark, Germany) and the mixture adapted to yield a viscosity of 3.5mPa.s. Hollow glass spheres with a mean size of 10 μm (Sphericel, Potters Industries, Parsippany, USA) were used as tracer particles and seeded into the fluid. A circulating heating pump was inserted into the fluid reservoir to ensure uniform distribution of the glass spheres at a temperature of 37°C.

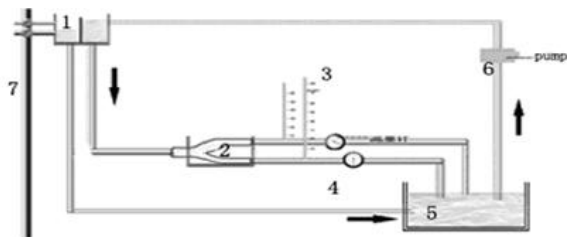


Figure 2. the schematic diagram of the vascular model recirculation system

1.upstream reservoir, 2. carotid bifurcation model, 3. manometer, 4. flow meter 5. downstream reservoir, 6. centrifugal pump, 7. slide pole

The PIV measurements were taken at five different flow rates which were shown in Table1. These five different work conditions were in behalf of the low velocity, mean velocity, peak velocity in the internal carotid artery and two high velocities for control study.

Table 1.The basic hydrodynamic parameters in five work condition

work condition	flow rate (ml/s)	mean velocity (m/s)
1	38.15	0.355
2	60.62	0.559
3	90.16	0.839
4	155.93	1.451
5	259.20	2.412

2.1 Particle image velocimetry

The PIV technique allows the instantaneous capture of an entire flow fields (Yu et al., 2007). A double pulsed Nd:Yag laser (NewWave, GeMini Y120-15,USA) with an energy of 50 mJ at a repetition rate of 15 Hz was used for illumination of a light sheet which was directed into the centerline of the fluid flow. The motion of the seeded particles was recorded twice by means of a CCD-Camera (TSI PowerView™ 4M, 630049-2, USA), which was positioned normal to the laser sheet. The time shift between the image acquisitions was 800 ms. The displacement of the particles between the two recorded images was directly proportional to the local fluid velocity. The images were analyzed using a cross-correlation algorithm yielding the local displacement vector for each interrogation area. In a frame-by-frame analysis the PIV measurements were obtained continuously, 200 frames were captured in each flow rate. The individual recordings were eventually used to reconstruct the flow field.

2.2 Numerical simulation

2.2.1 carotid bifurcation model

Gambit 2.0 software was used to create a geometric model and divide the grid. Altogether obtains non-structure hexahedron grid 51880. The experimental geometry of the model was shown in Figure3. The bifurcation angle is 45 °.

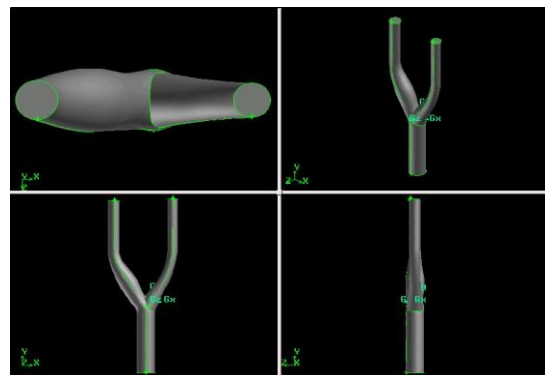


Figure 3. The numerical model of the carotid bifurcation

2.2.2 Controlling equations and calculation method

Suppose blood is isotropic, incompressible Newtonian fluid with constant density and viscosity, and assume that the vessel wall is rigid, impermeable, and the flow is unsteady. Excluding the volume force, heat exchange, and the other physical and chemical factors, the basic equations are:

$$\left\{ \begin{array}{l} \frac{\partial u_j}{\partial x_j} = 0 \\ \rho \frac{\partial u_j u_i}{\partial x_j} = -\frac{\partial P}{\partial x_i} + \mu \frac{\partial}{\partial x_j} \left(\frac{\partial u_i}{\partial x_j} + \frac{\partial u_j}{\partial x_i} \right) \end{array} \right.$$

The first one is the continuity equation, and the second is the equation of motion. u_i : flow field velocity, P : fluid pressure, ρ : fluid density, μ : viscosity.

Because of the basic equations are a set of strongly non-linear equations, we can only resort to the numerical methods. Finite Volume Method (FVM) is the main numerical method for solving such problems. FLUENT calculation software is the dedicated CFD software which is based on the finite volume method. Therefore, we choose the FLUENT6.1 software for numerical calculation.

2.2.3 Boundary Conditions

Using the speed entry and pressure exit as boundary condition; inlet velocity $u_{in} = Q/A$;

using non-slip flow boundary condition, the velocity components is zero. In the internal carotid and external carotid artery, the outlet pressures are zero. Solid wall boundary: the wall function.

2.2.4 Nine section to calculate the velocity

In the ICA, we divide it into nine sections evenly to show the velocity profile more elaborate, and to show the difference in different position within the ICA in different work condition.

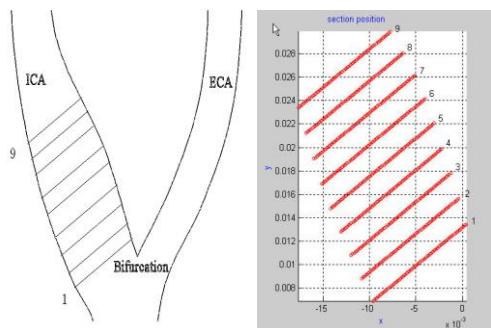


Figure 4. The nine sections for calculating the velocity in ICA.

3. Results

3.1. Velocity distribution in the horizontal section of internal carotid artery

The flow visualization revealed a high-velocity mainstream entering the ICA center, which divided and directed towards the inside wall. In the ICA a large area of flow separation developed near the outside wall. Inside this separation one anticlockwise

flowing vortex developed in work condition 1, 2 and 3. The location and scope of the vortex changed with the velocity. The higher the velocity was, the smaller the vortex scope was, and the farther the location to the bifurcation was. These phenomena were not significant in work condition 4 and 5. In work condition 1, the flow rate in boundary of the vortex was 0.0566 ± 0.0121 m/s; the flow rate in the middle of the flow separation was 0.1896 ± 0.0132 m/s. In work condition 2, the flow rate in boundary of the vortex was 0.0954 ± 0.0271 m/s; the flow rate in the middle of the flow separation was 0.2254 ± 0.0715 m/s. In work condition 3, the flow rate in boundary of the vortex was 0.1285 ± 0.0369 m/s; the flow rate in the middle of the flow separation was 0.2507 ± 0.0429 m/s. All the velocities were lower than the main stream velocity. And according to the equation

$\tau = \rho \overline{u'_i v'_j}$, we could know that in the outside wall of ICA where there were the vortex. The shear stress was low compared to the other zones.

3.2 Velocity distribution in ICA by numerical simulation

The numerical simulation also found there was one anticlockwise vortex, from section 1 to section 7 it became larger and larger. But in the same section, the largest vortex existed in work condition 1, 2 and 3. In the controlled high flow rate (work condition 4 and 5), although there was the vortex, its scope was smaller compared with the other work conditions. In the section 1, 2 and 3, the fastest velocity of the anticlockwise vortex was almost zero in work condition 1, 2 and 3; but in work condition 4 and 5, the velocity reached to 1 m/s. In section 4, 5 and 6, although the scope of the vortex was larger, the velocity was smaller compared with section 1, 2 and 3, that show which was just the core of the vortex. The largest anticlockwise vortex appeared in section 6, and that just the center of the sinus of the internal carotid artery. Between the anticlockwise vortex and mainstream that was where the flow separation was. Its location also changed with the flow rate, when the flow rate increased its location became farther and farther to the outside wall. But in section 8 and 9, this separation disappeared.

From these graphs, we could find that at the border of the anticlockwise vortex, the velocity was less than 0.5 m/s in work condition 1, 2 and 3. Even in work condition 4 and 5, the velocity was less than 1 m/s. And we could conclude the wall shear stress in this zone was low.

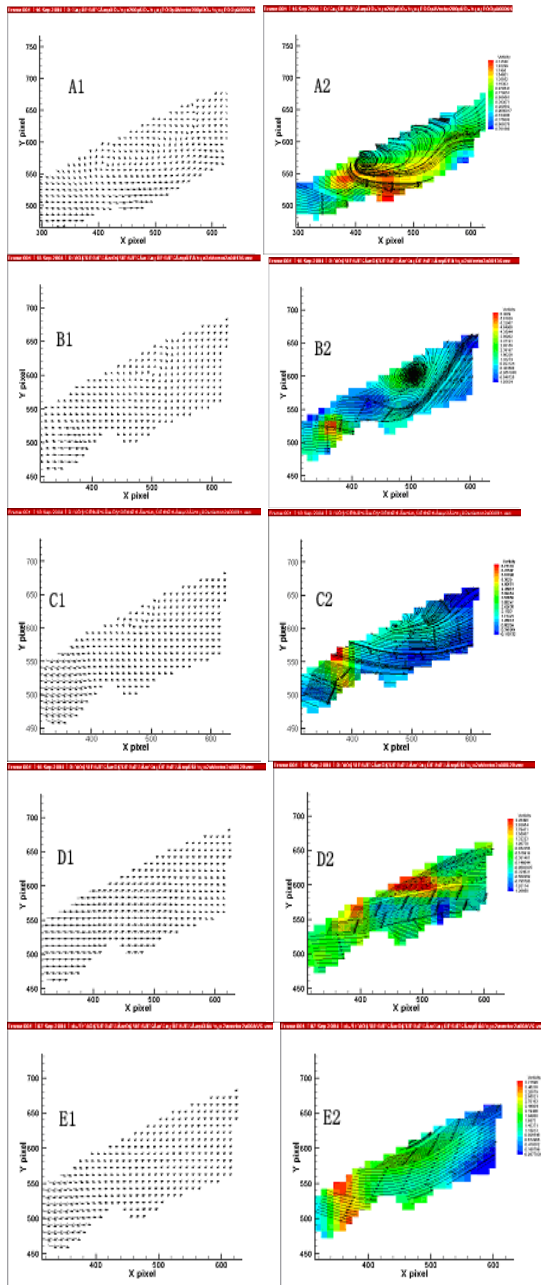


Figure 5. the velocity vectorgram and the vorticity map of horizontal section. (A1,A2)workcondition1;(B1,B2)workcondition2;(C1, C2)workcondition3; A separation was found in ICA and a significant anticlockwise rotating vortex was found near the outside wall of ICA. (D1,D2)workcondition4; (E1,E2)workcondition5. There was no flow separation and vortex.

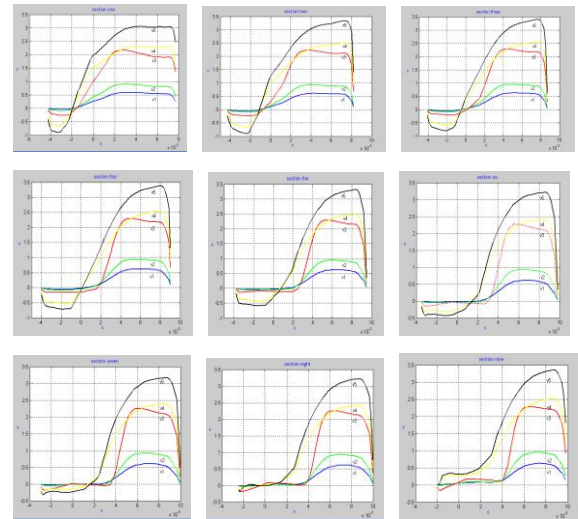


Figure 6. The velocity profile in nine sections under five work conditions. v1-v5: work condition1-workcondition5. From section1 to section6, there were flow separation and anticlockwise vortex. In section6,section7 and section8, there were no flow separation.

4. Discussions

Now, the standard hydrodynamic measuring method was laser doppler anemometry detection. But its defections must be noticed. First, it used one-point measuring technique which was tedious to perform spatial localization. Second, it was hard to provide enough information to describe the flow fields entirely in practical work. Third, it was time-consuming(Baldwin et al.,1994; Barbaro et al.,1998). In 1990s, a new hydrodynamic measuring method-PIV was developed, which based on the association of laser signal and fluid particles. Its merit lied in it could get 2D-velocity of the whole section in one imaging. So it was time-saving and not so tedious. What most important was it made people understand the whole flow fields in detail.Because the panel and area of the PIV image was stable, the PIV technique could implement overall and high-precision describe in small flow fields(Stamhuis and Videler,1995). So, in this research, PIV was used to describe the flow fields inside the model.

Despite the PIV method is more practical and time-saving, but the instrument is very expensive. So we think whether we can choose the other method which can get the similar result with the PIV? The numerical methods are very useful in supporting experimental methods and often enable the determination of flow variables which are difficult to obtain in experiments. So we choose the CFD to do numerical simulation.

The results of PIV demonstrated the flow directions were same with the main stream in CCA and their values are almost equal which proved the flow pattern was stable. In ICA flow separation presented and a vortex flow formed near the lateral wall. The scope and location of the vortex changed with the flow rate. The higher the flow rate was, the smaller the area was and the farther the distance to the bifurcation was. At last, in work condition 4 and 5, the vortex flow disappeared. In carotid sinus, there was always where the core of the vortex was in all of the five conditions.

Also, the numerical simulation we found in section 4, 5 and 6, although the scope of the vortex was larger, the velocity was smaller compared with section 1, 2 and 3, that show which was the core of the vortex, that can be used to explain why the atherosclerosis is prone to form in the sinus of ICA.

But whether in PIV or in numerical simulation, the velocity at the border of the anticlockwise vortex was low, and the wall shear stress must be low. So we decide that in ICA, at the site anticlockwise vortex formed, the wall shear stress was low. And because the atherosclerosis was prone to generate in these zones, we could also think about the relationship between the low shear stress and atherosclerosis.

Clinical observation and animal experiment discovered that early atherosclerotic lesions develop preferentially at bifurcations, branch points, and regions of high curvature in the arterial tree (Suo et al., 2008). This has led to a "geometric risk factor" hypothesis implicating local hemodynamic factors in atherogenesis (Friedman et al., 1983; Koch et al., 2009). Studies have generally implicated low wall shear stress (WSS) in atherogenesis: low shear stress could induce the expression of adhesion molecules ICAM-1 (Tsuboi et al., 1995), VCAM-1 (Varner et al., 1997), E-selectin (Hinds et al., 2001). And low shear stress could stimulate the MCP-1 expression (Shyy et al., 1994), and manipulate the synthesis and secretion of nitrogen monoxide (Dancu et al., 2007; McAllister et al., 2000). Otherwise in such zones, large macromolecules such as LDL deposit on the surface of endothelium, which make it have a long contact period with the endothelial cell (Wang et al., 2003; Deng et al., 1995). Through several pathways the macromolecules aggregated under the endothelium and were swallowed by macrophage cells. This was the early stage mark of atherosclerosis. In the low shear stress areas of the carotid artery, under the influence of low shear stress, many biochemical factors were secreted and stimulated. Also some harmful macromolecules accumulated in these zones, which may lead to or accelerate the atherosclerosis development.

In this study, we used PIV technique and numerical simulation method to measure the flow fields inside the modified model. The results confirmed there were flow separation and vortex flow and low wall shear stress zones in the ICA. This study supports the hypothesis that low shear stress led to the generation of atherosclerosis. And the model we used could supply a reliable experiment platform for future cell biology and molecular biology research.

Acknowledgements:

Authors are grateful to the State Key Laboratory of Hydraulics and Mountain River Engineering, Sichuan University, for financial and technological supports to carry out this work.

Corresponding Author:

Dr. Ye Meng

Department of Vascular Surgery of Renji Hospital
Shanghai Jiaotong University School of Medicine,
Shanghai 200127, China
E-mail: phdman@163.com

References

1. Ku DN, Giddens DP, Zarins CK, et al. Pulsatile flow and atherosclerosis in the human carotid bifurcation. *Arteriosclerosis* 1985; 5(3):293-302.
2. Lee D, Chiu JJ. Intimal thickening under shear stress in a carotid bifurcation—a numerical study. *Journal of Biomechanics* 1995; 29(1):1-11.
3. Rindt CC, Steenhoven AA. Unsteady flow in a rigid 3-D model of the carotid bifurcation. *Journal of Biomechanical Engineering* 1996; 118(1):90-96.
4. Ding ZR, Wang KQ, Lia J, et al. Flow field and oscillatory shear stress in a tuning-fork-shaped model of the average human carotid bifurcation. *Journal of Biomechanics* 2001; 34:1555-1562.
5. Ding ZR, Wang KQ. Tuning-fork-shaped model of the average human carotid bifurcation. *Shanghai Jiao Tong University Journal* 2002; 36(1):97-99.
6. Yu FX, Liao B, Shi YK, et al. Construction of an in vivo carotid artery bifurcation model. *Journal of Sichuan University* 2007; 38(6):1029-1032.
7. Baldwin JT, Deutsch S, Geselowitz DB, et al. LDA measurements of mean velocity and Reynolds stress fields within an artificial heart ventricle. *J Biomech Eng* 1994; 116(2): 190-200.
8. Barbaro V, Grigioni M, Daniele C, et al. Principal stress analysis in LDA measurement of

- the flow field downstream of 19-mm Sorin Bicarbon heart valve. *Technol Health Care*. 1998; 6(4): 259-70
9. Stamhuis E, Videler J. Quantitative flow analysis around aquatic animals using laser sheet particle image velocimetry. *J Exp Biol* 1995;198(Pt 2):283-94
 10. Suo J, Oshinski JN, Giddens DP. Blood flow patterns in the proximal human coronary arteries: relationship to atherosclerotic plaque occurrence. *Mol Cell Biomech* 2008;5(1):9-18
 11. Friedman MH, Deters OJ, Mark FF, et al. Arterial geometry affects hemodynamics. A potential risk factor for atherosclerosis. *Atherosclerosis* 1983; 46:225-231.
 12. Koch S, Nelson D, Rundek T, et al. Race-ethnic variation in carotid bifurcation geometry. *J Stroke Cerebrovasc Dis* 2009 ;18(5):349-53
 13. Tsuboi H, Ando J, Korenaga R, et al. Flow Stimulates ICAM-1 Expression Time and Shear Stress Dependently in Cultured Human Endothelial Cells. *Biochemical and Biophysical Research Communications* 1995;206(3):988-996
 14. Varner SE, Chappell DC, Alexander RW, et al. Endothelial VCAM-1 regulation by steady and oscillatory shear stress. *Atherosclerosis* 1997; 134(1-2):288.
 15. Hinds MT, Park YJ, Jones SA, et al. Local hemodynamics affect monocytic cell adhesion to a three-dimensional flow model coated with E-selectin. *Journal of Biomechanics* 2001; 34(1):95-103.
 16. Shyy YJ, Hsieh HJ, Usami S, et al. Fluid shear stress induces a biphasic response of human monocyte chemotactic protein-1 gene expression in vascular endothelium. *Proc Natl Acad Sci U S A* 1994; 91: 4678–4682
 17. Dancu MB, Berardi DE, Vanden Heuvel JP, et al. Atherogenic endothelial cell eNOS and ET-1 responses to asynchronous hemodynamics are mitigated by conjugated linoleic acid. *Ann Biomed Eng* 2007;35(7):1111-9
 18. McAllister TN, Du T, Frangos JA. Fluid Shear Stress Stimulates Prostaglandin and Nitric Oxide Release in Bone Marrow-Derived Preosteoclast-like Cells. *Biochemical and Biophysical Research Communications* 2000; 270,:643–648.
 19. Wang GX, Deng XY, Guidion R. Concentration polarization of macromolecules in canine carotid arteries and its implication for the localization of atherogenesis. *Journal of Biomechanics* 2003; 36(1):45-51.
 20. Deng XY, Marois Y, How T, et al. Luminal surface concentration of lipoprotein (LDL) and its effect on the wall uptake of cholesterol by canine carotid arteries. *J Vasc Surg* 1995; 21: 135-145.

7/31/2012